ARTICLE
Journal of Cellular Biochemistry 113:282–292 (2012)

Journal of Cellular Biochemistry

Glucose-Activated RUNX2 Phosphorylation Promotes Endothelial Cell Proliferation and an Angiogenic Phenotype

Adam D. Pierce,[1,2] Ian E. Anglin,[2] Michele I. Vitolo,[2] Maria T. Mochin,[2] Karen F. Underwood,[2] Simeon E. Goldblum,[3] Sravya Kommineni,[1] and Antonino Passaniti[2,4,5*]

[1] *The Graduate Program in Life Sciences (GPILS), University of Maryland School of Medicine, Baltimore, Maryland 21201*

[2] *The Marlene & Stewart Greenebaum Cancer Center, University of Maryland School of Medicine, Baltimore, Maryland 21201*

[3] *Department of Medicine and the Mucosal Biology Research Center, University of Maryland School of Medicine, Baltimore, Maryland 21201*

[4] *Department of Pathology, University of Maryland School of Medicine, Baltimore, Maryland 21201*

[5] *Department of Biochemistry & Molecular Biology, University of Maryland School of Medicine, Baltimore, Maryland 21201*

ABSTRACT

The runt-related protein-2 (RUNX2) is a DNA-binding transcription factor that regulates bone formation, tumor cell metastasis, endothelial cell (EC) proliferation, and angiogenesis. RUNX2 DNA binding is glucose and cell cycle regulated. We propose that glucose may activate RUNX2 through changes in post-translational phosphorylation that are cell cycle-specific and will regulate EC function. Glucose increased cell cycle progression in EC through both G2/M and G1 phases with entry into S-phase occurring only in subconfluent cells. In the absence of nutrients and growth factors (starvation), subconfluent EC were delayed in G1 when RUNX2 expression was reduced. RUNX2 phosphorylation, activation of DNA binding, and pRb phosphorylation were stimulated by glucose and were necessary to promote cell cycle progression. Glucose increased RUNX2 localization at focal subnuclear sites, which co-incided with RUNX2 occupancy of the cyclin-dependent kinase (cdk) inhibitor $p21^{Cip1}$ promoter, a gene normally repressed by RUNX2. Mutation of the RUNX2 cdk phosphorylation site in the C-terminal domain (S451A.RUNX2) reduced RUNX2 phosphorylation and DNA binding. Expression of this cdk site mutant in EC inhibited glucose-stimulated differentiation (in vitro tube formation), monolayer wound healing, and proliferation. These results define a novel relationship between glucose-activated RUNX2 phosphorylation, cell cycle progression, and EC differentiation. These data suggest that inhibition of RUNX2 expression or DNA binding may be a useful strategy to inhibit EC proliferation in tumor angiogenesis. J. Cell. Biochem. 113: 282–292, 2012.

KEY WORDS: TRANSCRIPTION; PHOSPHORYLATION; GLUCOSE; CELL CYCLE; ENDOTHELIAL CELL

Cancer cells acquire properties that promote tumor progression and metastasis, including the ability to recruit stromal cells and blood vessels (angiogenesis) [Kerbel, 2008]. Angiogenic factors produced by tumors induce quiescent vascular endothelial cells (EC) lining the blood vessels to proliferate and invade the tumor stroma (angiogenic switch), thus initiating the angiogenic response. Inhibitors of EC proliferation inhibit angiogenesis and the growth of tumors while pharmacological interventions that inhibit

Abbreviations: Ad, adenoviral; cdk, cyclin-dependent kinase; ChIP, chromatin immunoprecipitation; DN, dominant negative; EC, endothelial cell; IF, immunofluorescence; IP, immunoprecipitation; KO, knockout; pRb, phosphorylated retinoblastoma protein; RUNX2, runt-related transcription factor-2 (lower case for non-human protein); VEGF, vascular endothelial growth factor; WB, Western blotting; WT, wild type.

The authors declare no competing interests. None of the authors have a competing financial interest in any companies providing reagents for this study.

Additional Supporting Information may be found in the online version of this article.

Grant sponsor: NIH (NCI); Grant number: RO1 CA108846; Grant sponsor: AHA; Grant number: 09GRNT2130014; Grant sponsor: NIH (NIDDK); Grant number: P30 DK072488.

*Correspondence to: Antonino Passaniti, Departments of Pathology and Biochemistry & Molecular Biology, University of Maryland School of Medicine, 655 W Baltimore Street, Baltimore, MD 21201, USA. E-mail: apass001@umaryland.edu

Received 30 August 2011; Accepted 1 September 2011 • DOI 10.1002/jcb.23354 • © 2011 Wiley Periodicals, Inc.
Published online 12 September 2011 in Wiley Online Library (wileyonlinelibrary.com).

angiogenesis also inhibit EC proliferation [Folkman, 2007]. One mechanism controlling the shift in the balance of angiogenesis inhibitors and stimulators is activation of specific transcription factors that alter the expression of genes required for EC migration, proliferation, and differentiation thereby regulating angiogenesis [Semenza, 2003].

Runt-related (Runx) genes regulate a variety of developmental events including stem cell self-renewal and bone formation [Karsenty, 2001; Nimmo et al., 2005]. RUNX2 also regulates angiogenesis during development to activate the expression of vascular endothelial growth factor (VEGF) in hypertrophic chondrocytes and mesenchymal cells to promote local angiogenesis essential for bone formation [Zelzer et al., 2001; Kwon et al., 2011]. Targeted knockout (KO) of Runx2 results in dilated placental vessels, failure to vascularize the cartilaginous shaft, and smaller mice [Zelzer et al., 2001]. Wound healing responses in older Runx2 heterozygote KO mice are also severely compromised, reflective of angiogenic deficits [Tsuji et al., 2004]. Observations from Runx2 transgenic mice [Blyth et al., 2005] and our results that RUNX2 promotes cell transformation in cooperation with the Yap transcriptional coactivator (a c-yes associating protein) [Vitolo et al., 2007], indicate that RUNX2 is involved in regulating cell proliferation and oncogenesis. Dominant negative (DN) inhibition of RUNX2 inhibits angiogenesis [Namba et al., 2000; Sun et al., 2001] and breast cancer metastasis [Barnes et al., 2004], while over-expression of RUNX2 in EC [Sun et al., 2004] and breast tumor cells [Pratap et al., 2006] regulates cell proliferation, thereby enhancing blood vessel formation and tumor growth. Several RUNX2 target genes, including the metalloproteinases MMP7, MMP9, and MMP13, and the matrix protein osteopontin [Inman and Shore, 2003; Pratap et al., 2005], are involved in mediating its tumorigenic and angiogenic activity. Anti-angiogenic agents also inhibit the expression of RUNX2 and some of its target genes (VEGF, MMP9), consistent with the role of RUNX2 as an angiogenic regulator [Fu et al., 2011].

We and others showed that RUNX2 is an enzymatic target of the G1 and the G2/M cyclin-dependent kinases, cdk4 and cdk1, respectively, which phosphorylate RUNX2 to increase DNA binding [Qiao et al., 2006; Shen et al., 2006; Rajgopal et al., 2007]. During G2 cell cycle progression, RUNX2 associated with cyclin B1 complexes and was phosphorylated by cdk1 at a specific site in the C-terminal domain [Qiao et al., 2006]. EC utilize glucose as an energy source during proliferative angiogenesis [Vander Heiden et al., 2009] and RUNX2 DNA-binding and transcriptional activity are sensitive to glucose treatment [D'Souza et al., 2009]. Euglycemic, but not hyperglycemic (HG), levels of glucose-activated RUNX2 DNA-binding through endogenous production of IGF1 and the PI3K/ERK pathways. RUNX2 activity was essential for EC wound healing in response to glucose. Therefore, we hypothesized that glucose might promote specific RUNX2 phosphorylation events to regulate cell cycle progression. We now find that expression of a phosphorylation site-specific mutant of RUNX2 (S451A.RUNX2) results in inhibition of EC proliferation, wound healing, and EC differentiation (in vitro tube formation) in response to glucose, supporting a role for glucose-mediated RUNX2 phosphorylation in angiogenesis.

MATERIALS AND METHODS

REAGENTS, CELL CULTURE, AND EC BIOLOGICAL ASSAYS

Human bone marrow ECs are RUNX2-positive cells obtained from Dr. Ken Pienta and cultured in DMEM supplemented with 10% FBS. EC monolayer wound-healing assays were performed in defined serum-free medium with or without 5 mM D-glucose or Cdk4-selective inhibitor II (NSC625987) from EMD Biosciences (Darmstadt, GE), as described [Qiao et al., 2006]. EC tube formation (a measure of angiogenic activity) was determined by culturing 5×10^4 ECs in 96-well tissue culture plates coated with 50 μl of matrigel per well. Tube formation was expressed as the mean number of nodes per well, with nodes defined as the intersection of at least three tubular structures. EC proliferation assays were performed in 96-well tissue culture plates with EC expressing WT or mutant (S451A).RUNX2 at a density of 10,000 cells per well and measuring cell growth after staining with crystal violet [D'Souza et al., 2009].

CELL CYCLE ANALYSIS

Cell cycle progression through G2/M and G1 phases was analyzed after double thymidine blockade and release, as described [Qiao et al., 2006]. Briefly, for synchronization at the G1/S boundary, cells were incubated in 2 mM thymidine for 16 h followed by an 8 h recovery and a second 16 h incubation in 2 mM thymidine. Cells were washed with phosphate-buffered saline (PBS), harvested by trypsinization, fixed in cold 70% ethanol, and stored at −20°C. Before analysis, ethanol was removed by centrifugation of the cell suspension. Cells were resuspended in 1 ml of phosphate-buffered saline containing 50 μg/ml propidium iodide, 0.1% Triton-X 100, and 20 μg/ml RNase A and incubated for 30 min at 37°C prior to FACS analysis (Greenebaum Cancer Center Core Facility). In some cases, cells were starved in the absence of serum and glucose for 16 h and released in 5 mM glucose for 12 h. Cell cyle distribution of cells in different phases of the cell cycle (subconfluent proliferative; starved growth arrested; confluent growth arrested; confluent, replated at 50% subconfluence) was also determined by FACS analysis using the FlowJo8.8.6 software.

IMMUNOPRECIPITATION (IP) AND WESTERN BLOT (WB) ANALYSIS

Nuclear proteins were isolated using NucBuster (EMD Biosciences, Darmstadt, GE). Protein concentration was determined with the Bio-Rad Protein Assay. Cell lysates (100 μg) were incubated at 4°C for 16 h with 2 μg antibody diluted in IP buffer (20 mM Tris, pH 7.5, 2 mM $CaCl_2$, 1% Triton X-100, and protease inhibitors). Complexes were precipitated with PureProteome Protein G magnetic beads (Millipore) according to the manufacturer's protocol. Protein was eluted from the beads with Glycine buffer, pH 3.0, resolved on 4–12% NU-PAGE gels (Invitrogen), and transferred to nitrocellulose membranes (Invitrogen). Phospho-Ser-CDK (Cell Signaling, Danvers, MA), RUNX2 (MBL, Woburn, MA) and Flag-tag or HA-tag (Convance, Inc., Princeton, NJ) antibodies were used. Blots were incubated with primary antibody followed by horseradish peroxidase-conjugated goat anti-mouse IgG (KPL, Gaithersburg, MD) and

developed with enhanced chemiluminescence (ECL, Amersham Pharmacia Biotech, Buckinghamshire, England). Antibodies recognizing $p21^{Cip1}$, $p27^{Kip1}$, or cyclin D1 were obtained from Cell Signaling (Danvers, MA).

IMMUNOFLUORESCENCE (IF) AND SUBCELLULAR FRACTIONATION

EC were cultured on glass cover slips for 24 h prior to thymidine blockade and release with glucose. To detect endogenous RUNX2, cells were fixed with 3.7% formaldehyde, permeabilized with 0.25% Triton X-100 for 10 min, and blocked with 5% BSA/0.5% IGEPAL CA-630 (Sigma–Aldrich) in PBS for 1 h at room temperature. Slides were reacted with 1:50 diluted primary polyclonal anti-RUNX2 (M-70) antibody (Santa Cruz Biotechnology Inc, Santa Cruz, CA) for 16 h at 4°C. Secondary anti-rabbit AlexaFluor-488-conjugated antibody (2 μg/ml in PBS) was applied for 1 h and epifluorescence microscopy was performed. Hoechst stain (300 ng/ml) was used to visualize DNA. For subcellular fractionation of RUNX2, cells were lysed with hypotonic low salt buffer containing 0.5% Nonidet P-40. After centrifugation, the cytosolic (supernatant) fraction was saved and the pellet (nuclei) was extracted with high salt buffer (0.4 M KCl) and centrifuged to obtain the DNA-associated proteins (supernatant). The remaining pellet was extracted with 2% SDS-sample buffer to isolate RUNX2 associated with the chromatin fraction.

CHROMATIN IP ASSAYS

Chromatin IP (ChIP) assays utilized PCR primers targeting the $p21^{Cip1}$ promoter RUNX2 site-A (−2.2 kb). Non-specific IgG and antibody (nucleolin) were used for control IP. FACS analysis was used to confirm cell cycle blockade prior to ChIP. Cells were fixed with 1% formaldehyde, extracted with lysis buffer, sonicated, and clarified by centrifugation. IP of the supernatant with RUNX2-specific (Santa Cruz; M70) antibody was followed by PCR with primers specific for the distal RUNX site in the proximal promoter. $p21^{Cip1}$ promoter site A primers were: 5′-GGGCAGAAGTCCTCCCTTAGAGTG-3′ (UP) 3′-CTCCCCGAAGTTCCGTCACCCTC-5′ (DOWN) for an anticipated product of 337 bp.

RNAi DESIGN AND RUNX2 GENE KNOCKDOWN

For transient, specific RUNX2 targeting, the Imgenex shRNA vectors subcloned into the pSupNeo vector were utilized, as described [Qiao et al., 2006]. Sequences targeted were: ggacgaggcaagagtttca(Rx3); ccataaccgtcttcacaaa(Rx2); ccacaaggacagagtcaga(Rx1); ggatgaatctgtttggcga(Rx4). Control GFP Target Site: tctgtgtgtttgactctga. For specific $p21^{Cip1}$ knockdown, shRNA targeting the p21cDNA from the CDKN1A gene ($p21^{Cip1}$), NM078467: (ttagtctcagtttgtgtgtcttaattatt) were constructed as described for RUNX2. EC were transfected with the Qiagen Trans-Messenger reagents and mRNA expression was measured by qRT-PCR using RUNX2-specific (forward: 5′-GCACAGACAGAAGCTTGAT-3′; reverse: 5′-CCCAGTTCTGAAGCACCT-3′), $p21^{Cip1}$-specific (forward: 5′-CCGAAGTCAGTTCCTTGTGG-3′; reverse: 5′CCGCCATTAGCGCATCACAG-3′), or GAPDH-specific primers (forward: 5′CCGTCTAGAAAAACCTGCCAA-3′; reverse: 5′TGTAGCCAAATTCGTTGTCATACC-3′) and SYBR green detection. For stable RUNX2 knockdown, the Mission Lentiviral system (Sigma–Aldrich) was used to target five different sites within the RUNX2 coding sequence: gctacctatcacagagcaatt (TRC653); ctcagtgatttagggcgcattc (TRC 654); gtggtcctatgaccagtctta (TRC 656); tgcactatccagccacctttact (TRC 657); cagcactccatatctctact (TRC 655).

RUNX2 EXPRESSION VECTORS

The full-length RUNX2 cDNA (a gift from Dr. Y. Ito) was subcloned into the pCMV-tag2a vector (Stratagene) as described [Sun et al., 2004]. The Flag-tag S451A.RUNX2 mutant was prepared by site-directed mutagenesis as described [Qiao et al., 2006]. Flag-tag RUNX2 or Flag-tag DN-RUNX2 (missing exon8) was subcloned into the pShuttle vector (Clontech) before restriction enzyme cloning into the adenoviral (Ad) Adeno-X vector (BD Biosciences, Palo Alto, CA). The dominant negative activity of RUNX2Δ8 was quantified using $p21^{CIP1}$ promoter-luciferase assays [Sun et al., 2004]. Ad vectors were prepared in HEK293 packaging cells by sequential transfection/infection and viral titers of HEK293 supernatants were determined by cell lysis.

ELECTROPHORETIC MOBILITY SHIFT ASSAYS (EMSA)

A traditional EMSA was used for RUNX2 DNA binding as described [D'Souza et al., 2009]. Nuclear extracts were isolated using a low salt/high salt method and incubated at room temperature with a (^{32}P)-labeled osteocalcin promoter oligonucleotide (−141 to −165): 5′-CGTATTAACCACAATACTCG-3′.

DNA-BINDING ENZYME-LINKED IMMUNOSORBENT ASSAY (D-ELISA) PROTOCOL

DNA binding was quantified with a specific ELISA format method [Renard et al., 2001] as modified for RUNX2-specific detection (Underwood et al., 2011; unpublished data). Avidin-coated 96-well plates (Greiner Bio-One, Basel, Switzerland) were fixed with sodium carbonate for 2 h at 24°C. After rinsing 3× with wash buffer, a 3′-biotin labeled oligonucleotide, containing three osteocalcin RUNX2-binding sites, was added for 2 h. Nuclear extracts containing RUNX2 protein were exposed to the plate with rocking for 16 h at 4°C. Primary mouse antibody against RUNX2 (D130-3; MBL, Inc.) was added for 1 h at 24°C and secondary anti-mouse antibody-HRP for 30 min at 24°C. TMB substrate (50 μl) was allowed to react with the HRP in the dark. Once color development was confirmed, 50 μl of stop solution was added to each well and absorbance (A_{450nm}) was measured with a BioTrack II plate reader spectrophotometer (Amersham Biosciences/GE Healthcare, Piscataway, NJ).

STATISTICAL ANALYSIS

Results are expressed as the mean (±SD) of at least three replicate samples per data point. Experiments were repeated at least twice. For comparison of measurements relative to control samples, the Student's *t*-test was used to determine statistical significance. *P*-values <0.01 were considered significant. For comparison of multiple measurements, data were analyzed using Tukey's post hoc adjustment for 2-by-2 comparisons following ANOVA. *P*-values <0.05 were considered significant.

RESULTS

REGULATION OF CELL CYCLE PROGRESSION BY GLUCOSE-ACTIVATED RUNX2

We have found that cell cycle progression through the G2 phase is mediated by cdk1-dependent phosphorylation of RUNX2 [Qiao et al., 2006] and that glucose activates IGF1/IGFR signaling to increase RUNX2 DNA binding [D'Souza et al., 2009]. To determine whether ECs require glucose to enter and exit the G2 phase of the cell cycle, cell cycle arrest in G1/S was initiated with a double thymidine blockade followed by glucose treatment after removal of thymidine. Glucose addition (5 or 25 mM) promoted cell cycle progression out of S-phase, into G2/M and into G1 over a period of 12 h (Fig. 1A). In the absence of glucose or treatment with an inhibitor of glucose metabolism, 2-deoxyglucose (2-DG), cell cycle progression was delayed and exit from G1/S, entry into G2, and exit from G2 was incomplete. RUNX2 DNA-binding activity was stimulated by glucose with peak activity at 4 h (Supplementary Fig. S1). On the other hand, under nutrient and serum starved conditions, EC were blocked in G1/S, but 20% of the EC were in G2 (Supplementary Fig. S2A,B). In response to glucose, these confluent EC progressed through G2/M and entered G1 but did not progress beyond G1, consistent with contact inhibition [Qiao et al., 2006]. RUNX2 DNA-binding increased in response to glucose (Supplementary Fig. S3A) in the absence of changes in protein levels. Cell cycle-specific proteins did not indicate progression through G1 over the first 8h (Supplementary Fig. S3B). Expression of $p27^{Kip1}$, $p21^{Cip1}$, and cyclin D after 8h was consistent with cell cycle arrest at confluence. RUNX2 DNA-binding at later times (10–11 h) is consistent with the small number of cells delayed in G2 by starvation

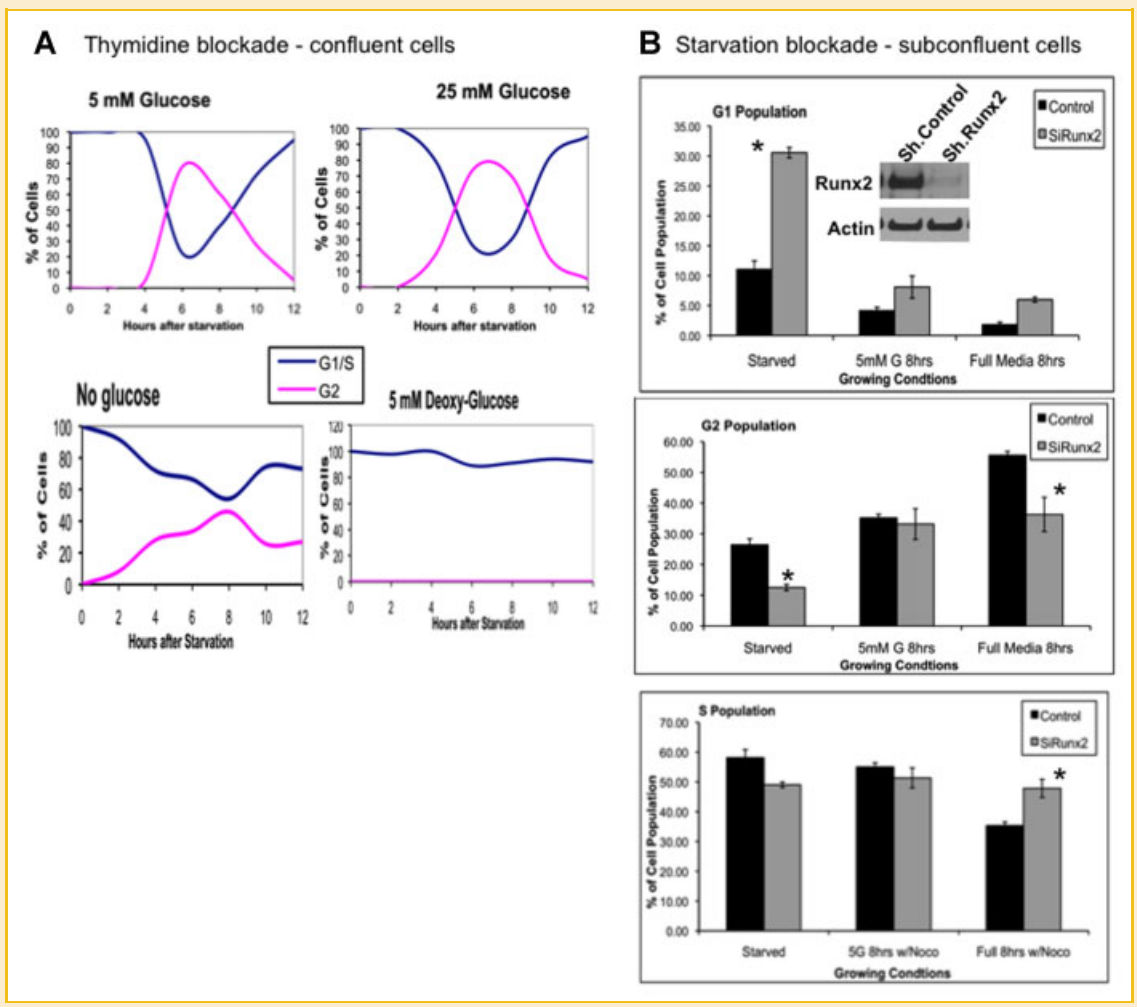

Fig. 1. Glucose-activated Runx2 DNA-binding and cell cycle progression through G2/M and G1 phases of the cell cycle. A: EC were synchronized at the G1/S transition after thymidine blockade (confluence) and released with 0, 5 mM, or 25 mM glucose or 5 mM 2-deoxyglucose. Propidium iodide-stained EC were detected by FACS analysis and the percentage of cells in each phase of the cycle was plotted. B: Cell cycle (G1, G2, S) profiles of subconfluent cells starved for 16 h and released in 5 mM glucose or full media (10% FBS, 25 mM glucose) for 8 h are shown from an experiment performed in triplicate. Subconfluent and starved cells infected with RUNX2-targeting shRNA lentivirus (gray bars) or control virus (black bars) were released from cell cycle blockade in the presence of nocodazole (0.2 μg/ml) to prevent mitotic exit and block re-entry into G1. *Inset:* Subconfluent cells were infected with RUNX2-targeting shRNA lentivirus or control virus and RUNX2 protein levels were confirmed by WB analysis (*differences for control vs. shRNA were significant ($P < 0.05$). [Color figure can be seen in the online version of this article, available at http://wileyonlinelibrary.com/journal/jcb]

(Supplementary Fig. S2A,B), which progressed into G1. Confluence prevented cell cycle progression of starved ECs while replating at subconfluence allowed progression (Supplementary Fig. S2C).

To determine whether RUNX2 might regulate cell cycle progression in response to glucose, subconfluent-starved cells in which RUNX2 was reduced with lentiviral shRNA were treated with glucose or complete media containing serum and growth factors. To focus on G1/S progression, cells in G2 were prevented from advancing through M-phase and into G1 with nocodazole. Starvation of cells in which RUNX2 was silenced resulted in increased G1 arrest and a decrease in G2/M, consistent with a reduced ability to progress into G2 (Fig. 1B; *starved*). After glucose treatment, RUNX2-positive or -knockdown cells progressed into G2/M. In complete medium (glucose and growth factors), entry into G2 was inhibited in RUNX2-knockdown cells, consistent with a delay in S-phase (Fig. 1B; *full media* **)**, suggesting a requirement for RUNX2 in growth factor-stimulated cell cycle progression.

RUNX2 PHOSPHORYLATION IN RESPONSE TO GLUCOSE

RUNX2 DNA-binding and transcriptional activity is regulated by cdk1 [Qiao et al., 2006; Rajgopal et al., 2007], cdk4 [Shen et al., 2006], and ERK-mediated [Ge et al., 2009] phosphorylation, but the direct modifications to RUNX2 in response to glucose are unknown. IP of nuclear extracts from EC with a phospho-Ser-CDK site antibody and WB for RUNX2 showed that endogenous RUNX2 protein in EC was phosphorylated in response to glucose (Fig. 2A,ii). Reciprocal IP of RUNX2 followed by WB with phospho-Ser-CDK site antibody showed a similar response, which was ablated by λ-phosphatase treatment, consistent with a phosphorylation event (Fig. 2A,iii*)*. RUNX2 containing a mutant cdk phosphorylation site, RUNX2 (S451A), exhibited reduced phosphorylation relative to WT-RUNX2 when expressed in HEK293 cells (Fig. 2B*)*. In these cells, total phospho-Ser CDK substrates were unaffected by RUNX2 overexpression (Fig. 2B; *Input, IP P-Ser*). Mutation of the RUNX2 cdk phosphorylation site also reduced DNA binding (Fig. 3A). In contrast, wild-type RUNX2 from EC bound DNA, but phosphatase treatment-reduced DNA binding. Glucose activates Cdk4 by upregulating expression of Cyclin D [Ryu et al., 2010]. RUNX2 activity in response to glucose was reduced by pretreatment with a selective Cdk4 inhibitor (Fig. 3B,i). Further, transfection of ECs with a dominant-negative CDK4 expression vector (DN-CDK4) dose-dependently inhibited RUNX2 activity (Fig. 3B,ii). To establish whether cdk4 was glucose responsive, a Cdk phosphorylation site (Ser795) on retinoblastoma, pRb, was monitored [Kitagawa et al., 1996]. WB detected phospho-Ser795 pRb within 3-4h after glucose treatment (Fig. 3B,iii). These results are consistent with cdk4 operating as an upstream kinase in the glucose-mediated signal transduction cascade activating RUNX2.

GLUCOSE-ACTIVATED RUNX2 PHOSPHORYLATION AND SUBNUCLEAR LOCALIZATION

Sites of focal RUNX2 subnuclear staining coincide with active transcriptional complexes [Harrington et al., 2002]. To determine if glucose alters RUNX2 subnuclear localization, EC were blocked in

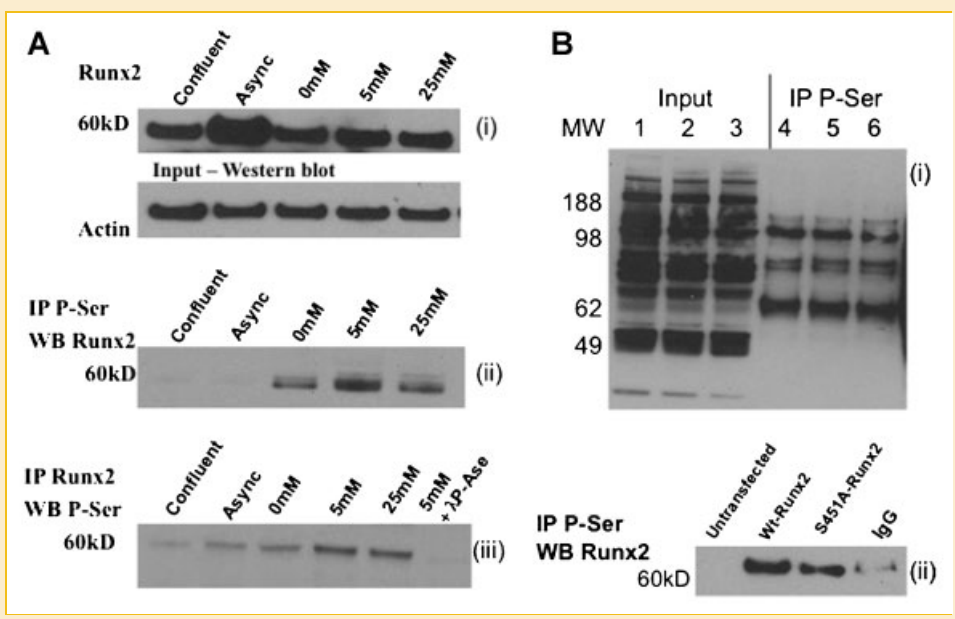

Fig. 2. Glucose regulates phosphorylation of a RUNX2 cdk target site. A: Endogenous RUNX2 protein was isolated from asynchronous (Async) or confluent EC or from cells starved and treated with glucose as indicated (i). RUNX2 was detected after IP with phosphoserine-CDK-substrate (P-Ser) antibody (ii) or P-Ser was detected after IP with RUNX2-specific antibody (iii). B: Detection of phospho-serine CDK sites in transfected HEK293 cells (i). Cells were untransfected (lanes 1,4) or transfected with cDNA vector expressing WT-RUNX2 (lanes 2,5) or a mutant CDK phosphorylation site RUNX2, Runx2.S451A (lanes 3,6). Total nuclear extracts were probed with a phospho-Ser CDK site antibody before (Input; lanes 1, 2, 3) or after immunoprecipitation with phospho-Ser antibody (IP P-Ser; lanes 4, 5, 6). Levels of phospho-Ser sites were similar in untransfected, WT-RUNX2 transfected, or S451A-Runx2 transfected cells. Molecular weight (MW) markers indicate kDa. Phosphorylation of WT-RUNX2 or RUNX2(S451A) mutant after P-Ser IP was measured in nuclear extracts from transfected HEK293 cells (ii). Non-specific IgG was used as negative control for IP of Wt-RUNX2 sample.

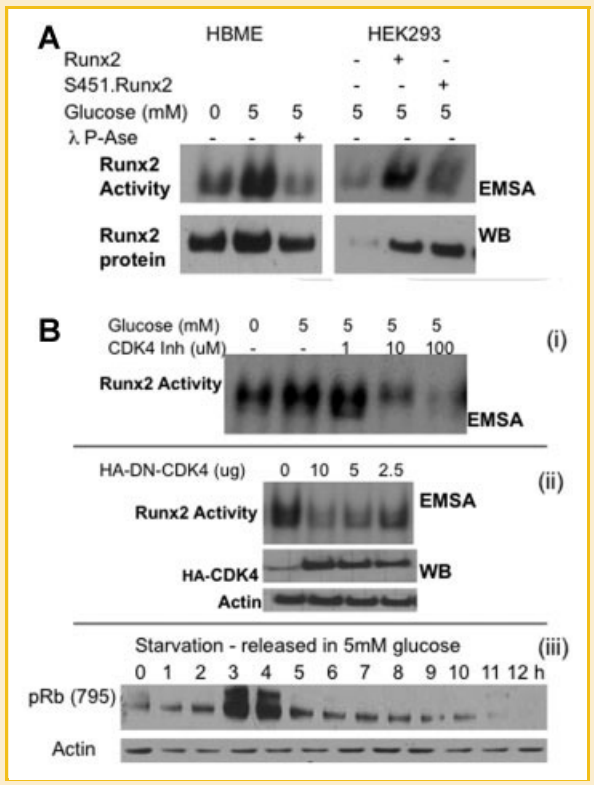

Fig. 3. Phosphorylation of RUNX2 in response to glucose is dependent on cdk4. A: Nuclear extracts from starved or glucose-treated cells were treated with λ-phosphatase prior to RUNX2 DNA-binding EMSA. DNA-binding activity from cells expressing WT-RUNX2 or RUNX2(S451A) was confirmed by EMSA. RUNX2 protein levels were confirmed by WB. B: CDK4 phosphorylates RUNX2 in response to glucose in the G1 phase of the cell cycle. EC were starved and treated with 0 or 5mM glucose or with 5 mM glucose and a selective CDK4 inhibitor (1, 10, and 100 μM) (i). In some cases, cells were transfected with a DN-CDK4 pMSCV plasmid (2.5, 5, and 10 μg) prior to isolation of nuclear extracts (ii). RUNX2 DNA-binding activity was determined by EMSA. Phosphorylated-Retinoblastoma (pRb) protein (a substrate of active Cdk4 complex) was used to confirm cdk4 activity (iii). pRb was detected by WB with antibody specific for phospho-Rb(Ser795).

G1/S by serum, glucose, and growth factor starvation and released into G2 with glucose. By IF, focal staining of RUNX2 protein was observed within 4 h after treatment, with reduced staining after 8 h (Fig. 4A,B). Biochemical fractionation and WB analysis confirmed that RUNX2 protein and activity were localized to the nucleus even in the absence of glucose treatment (Fig. 4C), thus supporting a subnuclear relocalization in response to glucose.

Focal localization of nuclear RUNX2 in response to glucose may indicate regulation of specific RUNX2 target genes. The cdk inhibitor, $p21^{Cip1}$, which regulated EC proliferation (Supplementary Fig. S4) is repressed at the promoter level by RUNX2 [Westendorf et al., 2002; Sun et al., 2004]. RUNX2 knockdown resulted in elevated $p21^{Cip1}$ mRNA levels as measured by Q-RTPCR (Supplemetary Fig. S5). $TGF\beta_1$ induces $p21^{Cip1}$ but RUNX2 inhibited $p21^{Cip1}$ expression in response to $TGF\beta_1$ while a DN-RUNX2 did not (Supplementary Fig. S6). The $p21^{Cip1}$ promoter contains three consensus RUNX2 interaction sites: A, B, and C (Fig. 5A). To determine which site was the preferred functional-binding site, oligonucleotides corresponding to each site were synthesized and examined as competitors for RUNX2 DNA binding. RUNX2 binding sites A and C exhibited significant interaction with RUNX2 relative to the osteocalcin promoter site using traditional EMSA (Fig. 5B) or a new DNA-binding ELISA, D-ELISA, (Fig. 5C). Consistent with these results, glucose treatment after thymidine block and release resulted in recruitment of RUNX2 protein to $p21^{Cip1}$ site A in vivo as determined by ChIP assay (Fig. 5D).

FUNCTIONAL CONSEQUENCES OF GLUCOSE-REGULATED RUNX2 ACTIVITY

A conserved RUNX2 cdk-consensus site Serine-451(472) found in the C-terminal region (GDRSPSRM; cdk site in bold; underlined phospho-Ser) regulates DNA-binding[Qiao et al., 2006; Shen et al., 2006; Rajgopal et al., 2007]. To explore the functional consequences of this specific phosphorylation site, a mutant RUNX2(S451A) protein that cannot be phosphorylated was ectopically expressed in EC that express endogenous WT-RUNX2. Ectopic WT-RUNX2 was expressed in control cells. Proliferating, but not growth arrested, EC differentiate on extracellular matrix (matrigel), a model of angiogenesis, if they express RUNX2 and are actively cycling (subconfluent) prior to transfer to matrigel [Sun et al., 2004]. EC were harvested while subconfluent and their ability to differentiate into tube-like structures was measured. EC expressing WT-RUNX2 formed differentiated tubular networks when cultured on matrigel while expression of mutant RUNX2 (S451A) was very effective at inhibiting tube formation in cells in which glucose metabolism was blocked (Fig. 6A). EC tube formation depends on active migration. We showed that RUNX2 is required for EC migration in a wounded monolayer assay [D'Souza et al., 2009]. To determine whether cdk4 phosphorylation, which activates RUNX2 DNA binding (Fig. 2C), regulates EC migration, EC were treated with a cdk4-selective inhibitor. After 18 h, untreated cells had closed almost 70% of the wounded monolayer, whereas inhibition of cdk4 inhibited wound closure by about one-half (35% wound closure) in response to glucose (Fig. 6B). Mutation of the RUNX2 cdk site also affected EC migration and wound healing since EC expressing RUNX2(S451A) exhibited decreased wound closure in response to glucose relative to cells expressing WT-RUNX2 (Fig. 6C). Inhibition of wound closure may be partially due to effects on cell proliferation. Therefore, cells expressing the RUNX2(S451A) mutant were tested for their proliferative capacity, which was also reduced after 3–5 days relative to WT-RUNX2 transfected cells (Fig. 6D).

DISCUSSION

Results from this study provide evidence for the glucose-dependent regulation of RUNX2 DNA-binding activity through cell cycle-specific post-translational modifications. Previous findings had established that euglycemic levels of glucose increased, whereas hyperglycemic levels repressed, RUNX2 DNA-binding and transcriptional activity in microvascular EC [D'Souza et al., 2009]. RUNX2 can also regulate cell cycle progression [Galindo et al., 2005; Qiao et al., 2006]. We now report that glucose promotes RUNX2 DNA

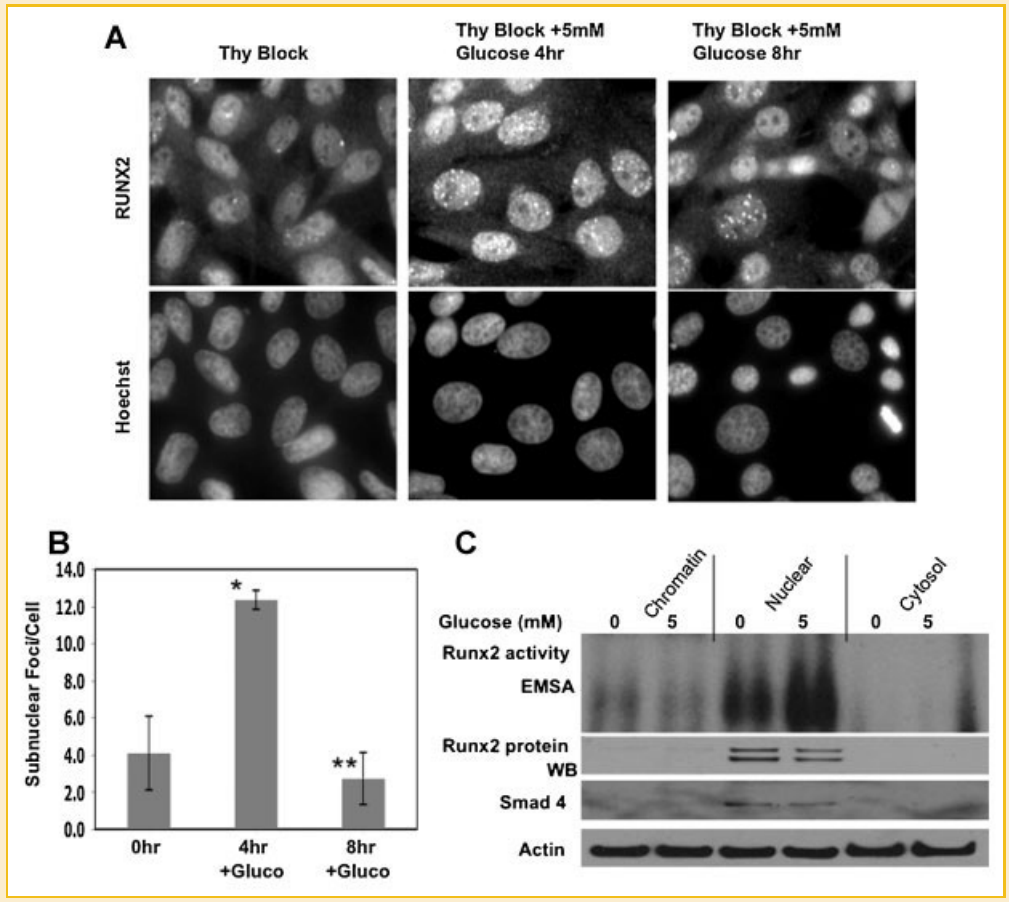

Fig. 4. RUNX2 activation and subnuclear localization in response to glucose. A: Cells were thymidine blocked prior to release with 5 mM glucose as in Figure 1. Subnuclear localization of RUNX2 was detected by IF using a RUNX2-specific antibody. Hoechst stain (300 ng/ml) was used to confirm nuclear localization. B: The number of nuclear foci was counted from three separate fields. $^{*}P < 0.03$ at 4 h; $^{**}P < 0.37$ at 8 h relative to untreated control (0 h). C: Subcellular localization of RUNX2 protein and DNA-binding activity in response to glucose. WB analysis was used to monitor RUNX2 protein in the nuclear, cytoplasmic, and chromatin extracts of glucose-treated (0, 5 mM) cells. Extracts were harvested as previously described. EMSA was performed to confirm Runx2 DNA-binding activity in each isolated fraction. Smad4 was used as a marker for isolated nuclei. Actin was detectable in all fractions and used as a loading control.

binding and cell cycle progression in vascular EC through phosphorylation of a specific cdk-consensus site on RUNX2. This phosphorylation site has been shown to be a substrate of both G2/M (cdk1) and G1 (cdk4) protein kinases. In addition, glucose treatment promoted changes in RUNX2 subnuclear localization, which were associated with activation of the cell cycle-regulated RUNX2 target gene $p21^{Cip1}$. Further support of a role for RUNX2 phosphorylation in EC function was obtained with a RUNX2 cdk-phosphorylation site mutant, which inhibited EC tube formation (differentiation), wound healing, and proliferation.

GLUCOSE-DEPENDENT REGULATION OF RUNX2 PHOSPHORYLATION AND CELL CYCLE PROGRESSION

The RUNX2 DNA-binding protein is glucose-responsive and regulates cell cycle progression and expression of a variety of target genes in osteoblasts, tumor cells, and EC [Pratap et al., 2005; Qiao et al., 2006]. We find that glucose treatment activates RUNX2 DNA-binding and EC cycle progression, but targeted knockdown of RUNX2 delays progression in G2/M and G1 phases of the cell cycle (Fig. 1). RUNX2 was critical for G1 exit under starvation conditions and for growth factor-dependent entry into G2, but glucose promoted exit out of G1 and entry into G2 regardless of RUNX2 expression. These results are consistent with previous reports that IGF1 activates RUNX2 in EC to increase proliferation and DNA synthesis while the G2/M-specific cyclinB/Cdk1 complex phosphorylates RUNX2 in response to IGF1 to promote cell cycle progression [Sun et al., 2004; Qiao et al., 2006; Rajgopal et al., 2007]. RNA interference reagents targeting RUNX2 delayed entry into and exit out of the G(2)/M phases of the cell cycle [Qiao et al., 2006] and RUNX2 was associated with cyclin B1 in mitotic EC. RUNX2 was phosphorylated at Ser(451) by cdk1 in these cells since cdk inhibition reduced RUNX2 DNA-binding in mitosis. The RUNX2 mutant S451A exhibited lower DNA-binding activity and reduced stimulation of anchorage-independent growth relative to wild-type RUNX2 [Qiao et al., 2006]. These published results and the current findings suggest that phosphorylation of RUNX2 by cdk1 facilitates cell cycle progression and promotes EC proliferation.

Cdk1-dependent phosphorylation events are also important in regulating mitotic RUNX2 activity in osteoblasts [Rajgopal et al., 2007]. When cells were blocked in mitosis and released to enter the

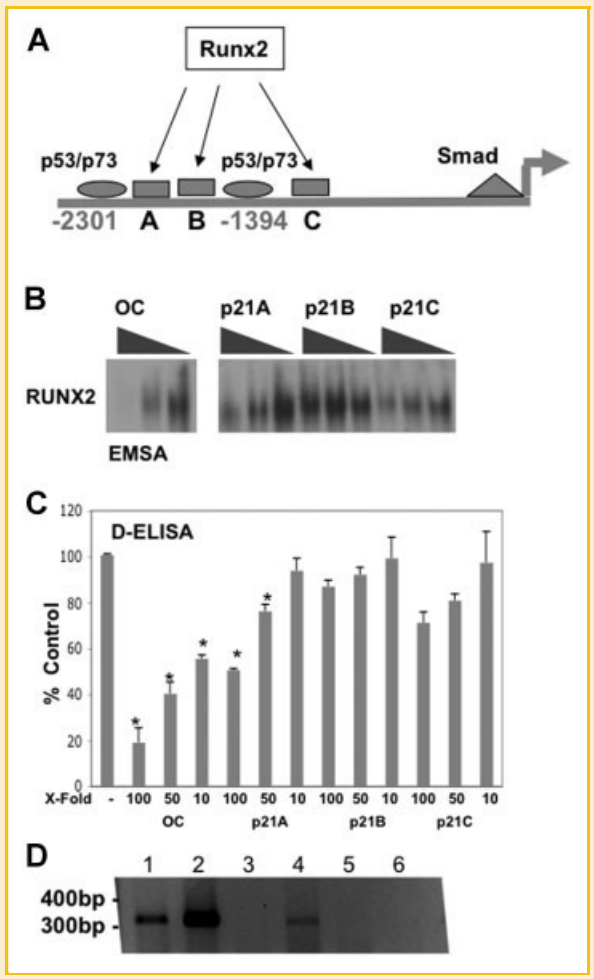

Fig. 5. Identification of a glucose-responsive RUNX2-binding site on the promoter of the RUNX2 target gene, $p21^{Cip1}$. A: p21Cip1 promoter site map. The p21Cip1 promoter contains two p53/p73 consensus interaction sites (⬭) and three Runx2 consensus-binding sites (▭) (ACACCAA) close to the distal p53/p73 sites. The proximal promoter contains consensus Smad-binding sites. B: RUNX2 DNA-binding EMSA: DNA oligonucleotides corresponding to $p21^{Cip1}$ promoter sites A, B, and C were used as competitors (*100×, 50×, 10×, indicated by triangles*) of radiolabeled osteocalcin (OC) promoter oligonucleotide recognizing RUNX2. C: RUNX2 DNA-binding ELISA: biotin-labeled OC promoter oligonucleotides were incubated with competing $p21^{Cip1}$ promoter site A, B, and C oligos at the indicated fold higher amounts (100×, 50×, 10×) relative to biotin-labeled oligos. Significant differences from untreated control were observed ($^*P < 0.05$). D: Chromatin IP (ChIP) assays used RUNX2-specific antibody and PCR primers specific for siteA of the $p21^{Cip1}$ promoter, which were validated with genomic DNA (*lane 1*) or input sheared DNA (*lane 2*). RUNX2 associated with $p21^{Cip1}$ promoter after glucose treatment (*lane 4*), but not in thymidine-blocked cells (*lane 3*). Negative controls include nucleolin antibody pull-down (*lane 5*) and non-specific IgG for pull-down (*lane 6*).

cell cycle, RUNX2 phosphorylation, which was phosphatase sensitive, also increased. Phosphorylated RUNX2 levels declined, however, when cells exited mitosis. It was suggested that the protein phosphatases PP1 and PP2A might be responsible for dephosphorylation events associated with cell cycle progression. Glucose treatment increased RUNX2 phosphorylation at a consensus cdk site (Figure 2), which was cdk4 regulated and is consistent with glucose activation of RUNX2 DNA-binding activity and pRb phosphorylation in the G1 phase of the cell cycle (Fig. 3). RUNX2 has been shown to interact with pRb itself and to promote cell differentiation [Berman et al., 2008; Calo et al., 2010]. In addition, cdk4 catalyzes RUNX2 phosphorylation at the same C-terminal site as cdk1, leading to RUNX2 activation, deacetylation, ubiquitination, and protein turnover [Shen et al., 2006]. Mutagenesis of the RUNX2 S472 site (equivalent to S451) increased the half-life of RUNX2 protein and reduced cyclin D1-induced RUNX2 degradation through the proteasome. The demonstration of cyclin D1-dependent RUNX2 turnover shows that RUNX2 activity may be closely tied to cell cycle events in osteoblasts and osteosarcoma cells.

It has been shown that Runx2 levels and function regulate G1 transition in MC3T3 preosteoblastic cells [Galindo et al., 2005] and that cell cycle control of Runx2 gene expression is impaired in osteosarcomas [San Martin et al., 2009]. Runx2 levels were cell cycle-regulated in MC3T3 preosteoblast cells. High expression was observed early in G(1) with low expression in early S phase and mitosis. Proteasome inhibition stabilized Runx2 protein levels in late G1 and S in MC3T3 cells, but not in osteosarcoma cells, which already expressed RUNX2 at high levels throughout the cell cycle. Thus, proteasomal degradation of RUNX2 was deregulated in osteosarcoma cells. Based on our current results in immortalized EC, RUNX2 regulation appears to be similar in transformed cells where protein levels do not change with growth arrest. Because DNA-binding activity is low and RUNX2 protein levels are stable in growth arrested EC, we focused on the post-translational (phosphorylation) aspects of RUNX2 activity. By examining glucose-dependent cell cycle progression in cells arrested in G1/S (with thymidine blockade or starvation), we found that cdk4-mediated RUNX2 phosphorylation is important in exit of EC from G1. Use of immortal EC may also model the activated EC found in the tumor microenvironment, which exhibit a dedifferentiated, mesenchymal phenotype [Potenta et al., 2008; Dudley and Klagsbrun, 2009].

FUNCTIONAL CONSEQUENCES OF GLUCOSE-ACTIVATED RUNX2 PHOSPHORYLATION

Glucose increased RUNX2 phosphorylation and promoted changes in subnuclear localization (Fig. 4), coincident with DNA binding and RUNX2 $p21^{Cip1}$ promoter occupancy (Fig. 5). The focal distribution of RUNX2 in these cells may indicate an association with transcriptional complexes [Harrington et al., 2002]. RUNX2 interacts with the transcriptional corepressor HDAC6 to inhibit $p21^{Cip1}$ promoter activity [Westendorf et al., 2002]. Similarly, recent reports have shown that RUNX2 colocalizes with active phospho-ERK on the promoters of RUNX2 target genes in differentiating osteoblasts [Li et al., 2010]. We observed that $p21^{Cip1}$ regulates EC proliferation (Supplementary Fig. S4) and that RUNX2 inhibits TGFβ-stimulated $p21^{Cip1}$ expression (Supplementary Fig. S6). Tumor cells lacking $p21^{Cip1}$ also proliferate in response to TGFβ, which induces a mesenchymal phenotype [Bachman et al., 2004]. These results suggest that $p21^{Cip1}$ and RUNX2 might act as key regulators of the cellular response to TGFβ in EC and tumor cells.

We have shown that RUNX2-dependent vascular remodeling in an EC wounded monolayer assay is reversed by specific inhibition of

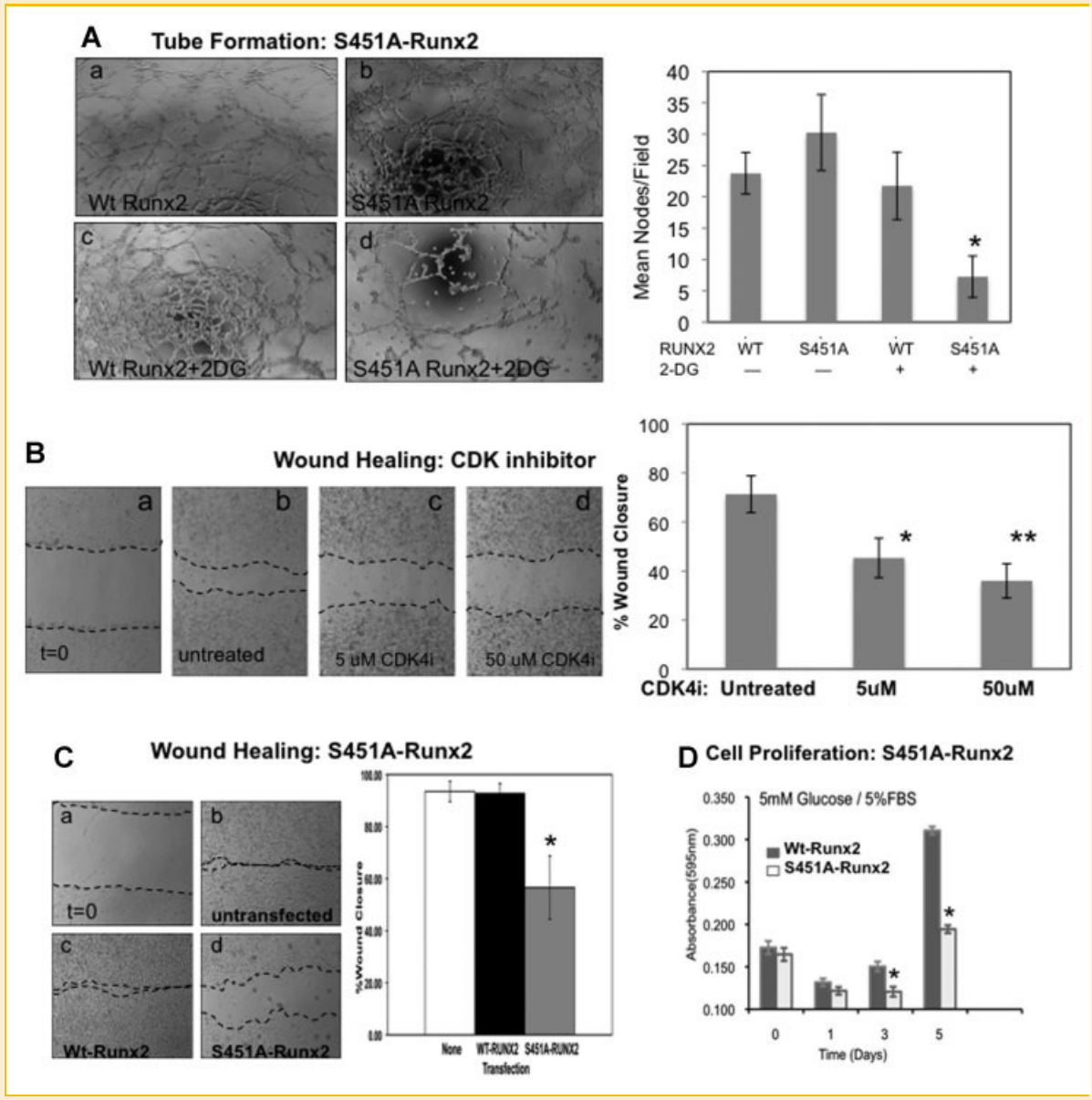

Fig. 6. RUNX2 phosphorylation regulates EC differentiation, wound healing, and proliferation in response to glucose. A: WT or mutant (S451A) RUNX2 was expressed in EC treated with or without 2-DG to induce partial chemical starvation. Tube formation was allowed to proceed for 4 h after plating on matrigel. Shown are representative photos. Each photographic field was separated into quadrants and the number of nodes per quadrant was counted: a node was defined as the intersection of at least 3 tubular projections. The mean (±SD) for each treatment is shown ($^{*}P < 0.006$ for S451A + 2DG vs. WT-RUNX2 + 2DG). B: Inhibition of CDK4 reduces EC wound healing. EC wound healing was examined in confluent cells either untreated (a,b) or treated (c,d) with a selective cdk4 inhibitor over an 18-h period. Dotted lines indicate extent of wound closure. Wound closure was defined relative to $t = 0$ (% wound closure). Quantitative wound closure was determined from at least three measurements per treatment ($^{*}P < 0.015$; $^{**}P < 0.004$ relative to untreated control). C: EC wound healing was measured in untransfected cells, cells transfected with WT-RUNX2 or cells transfected with mutant S451A-Runx2 vectors. Quantitative wound closure was determined from at least three independent measurements per treatment. $^{*}P < 0.028$ relative to untransfected control. D: Proliferation of EC expressing ectopic WT-RUNX2 or S451A.RUNX2 mutant was monitored over 5 days ($^{*}P < 0.05$ relative to wild-type RUNX2).

aldose reductase in hyperglycemia [D'Souza et al., 2009]. Euglycemia increases RUNX2 activity and promotes normal microvascular EC migration and wound healing, although the exact mechanism is not known. We now show that targeted knockdown of RUNX2 levels reduced cell cycle progression and that expression of the RUNX2(S451A) mutant inhibited EC tube formation (differentiation), wound healing, and proliferation (Fig. 6). These results reveal, for the first time, the functional importance of the RUNX2 cdk phosphorylation site in response to glucose. Other cdk substrates engineered with mutated phosphorylation sites can also act as antagonists and exhibit growth suppressing activity when ectopically expressed in cells [Antelman et al., 1997; Nair et al., 2010]. Mutation of cdk4 substrate sites in pRb resulted in cellular growth arrest in G1 [Antelman et al., 1997]. Cells stably expressing a PELP1 mutant with no CDK sites showed reduced response to estradiol and defects in cell cycle progression [Nair et al.,

2010]. These ''decoy'' substrate sites also inhibited phosphorylation of endogenous pRb and cell proliferation. Like PELP1, RUNX2 may mediate proliferative signals and promote cross talk with the cell cycle machinery. Phosphorylation of RUNX2 Ser-451 is a signal for protein ubiquitination, which leads to proteasomal degradation [Shen et al., 2006]. Therefore, the RUNX2(S451A) mutant could exert its anti-proliferative and anti-differentiation effects on EC because of reduced protein turnover and interaction with other cellular components. Although glucose activation at this specific cdk site can increase cell competence for tube formation, other RUNX2 phosphorylation sites may also be involved in regulating cell proliferation [Ge et al., 2009].

SUMMARY

Glucose promotes cell cycle progression in EC through both G2/M and G1 phases of the cell cycle, but entry into S-phase occurs only in subconfluent cells that can activate RUNX2 phosphorylation and nuclear relocalization, consistent with specific promoter occupancy. These studies define a relationship between glucose-activated RUNX2 phosphorylation, cell cycle progression, and EC differentiation. This relationship may have important implications for uncovering the mechanisms by which EC proliferation and angiogenesis regulate tumor growth in the tumor microenvironment.

ACKNOWLEDGMENTS

The authors appreciate the support of the Greenebaum Cancer Center CRF, the Graduate Program in Life Sciences, the Mid-Atlantic Nutrition Obesity Research Center (NORC) and other members of the laboratory (Brandon Cooper), and NORC (Dr. John McLenithan) for providing samples and advice. We also thank Drs. Rena Lapidus and Mariola Sadowska for assistance with the D-ELISA measurements. This article is subject to the NIH Public Access Policy.

REFERENCES

Antelman D, Perry S, Hollingsworth R, Gregory RJ, Driscoll B, Fung YK, Bookstein R. 1997. Engineered mutants of pRB with improved growth suppression potential. Oncogene 15:2855–2866.

Bachman KE, Blair BG, Brenner K, Bardelli A, Arena S, Zhou S, Hicks J, De Marzo AM, Argani P, Park BH. 2004. p21(WAF1/CIP1) mediates the growth response to TGF-beta in human epithelial cells. Cancer Biol Ther 3:221–225.

Barnes GL, Hebert KE, Kamal M, Javed A, Einhorn TA, Lian JB, Stein GS, Gerstenfeld LC. 2004. Fidelity of Runx2 activity in breast cancer cells is required for the generation of metastases-associated osteolytic disease. Cancer Res 64:4506–4513.

Berman SD, Yuan TL, Miller ES, Lee EY, Caron A, Lees JA. 2008. The retinoblastoma protein tumor suppressor is important for appropriate osteoblast differentiation and bone development. Mol Cancer Res 6:1440–1451.

Blyth K, Cameron ER, Neil JC. 2005. The RUNX genes: Gain or loss of function in cancer. Nat Rev Cancer 5:376–387.

Calo E, Quintero-Estades JA, Danielian PS, Nedelcu S, Berman SD, Lees JA. 2010. Rb regulates fate choice and lineage commitment in vivo. Nature 466: 1110–1114.

D'Souza DR, Salib MM, Bennett J, Mochin-Peters M, Asrani K, Goldblum SE, Renoud KJ, Shapiro P, Passaniti A. 2009. Hyperglycemia regulates RUNX2 activation and cellular wound healing through the aldose reductase polyol pathway. J Biol Chem 284:17947–17955.

Dudley AC, Klagsbrun M. 2009. Tumor endothelial cells have features of adult stem cells. Cell Cycle 8:236–238.

Folkman J. 2007. Angiogenesis: An organizing principle for drug discovery? Nat Rev Drug Discov 6:273–286.

Fu J, Wang W, Liu YH, Lu H, Luo Y. 2011. In vitro anti-angiogenic properties of LGD1069, a selective retinoid X-receptor agonist through down-regulating Runx2 expression on human endothelial cells. BMC Cancer 11:227.

Galindo M, Pratap J, Young DW, Hovhannisyan H, Im HJ, Choi JY, Lian JB, Stein JL, Stein GS, van Wijnen AJ. 2005. The bone-specific expression of Runx2 oscillates during the cell cycle to support a G1-related antiproliferative function in osteoblasts. J Biol Chem 280:20274–20285.

Ge C, Xiao G, Jiang D, Yang Q, Hatch NE, Roca H, Franceschi RT. 2009. Identification and functional characterization of ERK/MAPK phosphorylation sites in the Runx2 transcription factor. J Biol Chem 284:32533–32543.

Harrington KS, Javed A, Drissi H, McNeil S, Lian JB, Stein JL, Van Wijnen AJ, Wang YL, Stein GS. 2002. Transcription factors RUNX1/AML1 and RUNX2/Cbfa1 dynamically associate with stationary subnuclear domains. J Cell Sci 115:4167–4176.

Inman CK, Shore P. 2003. The osteoblast transcription factor Runx2 is expressed in mammary epithelial cells and mediates osteopontin expression. J Biol Chem 278:48684–48689.

Karsenty G. 2001. Minireview: Transcriptional control of osteoblast differentiation. Endocrinology 142:2731–2733.

Kerbel RS. 2008. Tumor angiogenesis. N Engl J Med 358:2039–2049.

Kitagawa M, Higashi H, Jung HK, Suzuki-Takahashi I, Ikeda M, Tamai K, Kato J, Segawa K, Yoshida E, Nishimura S, Taya Y. 1996. The consensus motif for phosphorylation by cyclin D1-Cdk4 is different from that for phosphorylation by cyclin A/E-Cdk2. Embo J 15:7060–7069.

Kwon TG, Zhao X, Yang Q, Li Y, Ge C, Zhao G, Franceschi RT. 2011. Physical and functional interactions between Runx2 and HIF-1alpha induce vascular endothelial growth factor gene expression. J Cell Biochem 2011, July 25, Epub ahead of pring.

Li Y, Ge C, Franceschi RT. 2010. Differentiation-dependent association of phosphorylated extracellular signal-regulated kinase with the chromatin of osteoblast-related genes. J Bone Miner Res 25:154–163.

Nair BC, Nair SS, Chakravarty D, Challa R, Manavathi B, Yew PR, Kumar R, Tekmal RR, Vadlamudi RK. 2010. Cyclin-dependent kinase-mediated phosphorylation plays a critical role in the oncogenic functions of PELP1. Cancer Res 70:7166–7175.

Namba K, Abe M, Saito S, Satake M, Ohmoto T, Watanabe T, Sato Y. 2000. Indispensable role of the transcription factor PEBP2/CBF in angiogenic activity of a murine endothelial cell MSS31. Oncogene 19:106–114.

Nimmo R, Antebi A, Woollard A. 2005. mab-2 encodes RNT-1, a *C. elegans* Runx homologue essential for controlling cell proliferation in a stem cell-like developmental lineage. Development 132:5043–5054.

Potenta S, Zeisberg E, Kalluri R. 2008. The role of endothelial-to-mesenchymal transition in cancer progression. Br J Cancer 99:1375–1379.

Pratap J, Javed A, Languino LR, van Wijnen AJ, Stein JL, Stein GS, Lian JB. 2005. The Runx2 osteogenic transcription factor regulates matrix metalloproteinase 9 in bone metastatic cancer cells and controls cell invasion. Mol Cell Biol 25:8581–8591.

Pratap J, Lian JB, Javed A, Barnes GL, van Wijnen AJ, Stein JL, Stein GS. 2006. Regulatory roles of Runx2 in metastatic tumor and cancer cell interactions with bone. Cancer Metastasis Rev 25:589–600.

Qiao M, Shapiro P, Fosbrink M, Rus H, Kumar R, Passaniti A. 2006. Cell cycle-dependent phosphorylation of the RUNX2 transcription factor by cdc2 regulates endothelial cell proliferation. J Biol Chem 281:7118–7128.

Rajgopal A, Young DW, Mujeeb KA, Stein JL, Lian JB, van Wijnen AJ, Stein GS. 2007. Mitotic control of RUNX2 phosphorylation by both CDK1/cyclin B

kinase and PP1/PP2A phosphatase in osteoblastic cells. J Cell Biochem 100:1509–1517.

Renard P, Ernest I, Houbion A, Art M, Le Calvez H, Raes M, Remacle J. 2001. Development of a sensitive multi-well colorimetric assay for active NFkappaB. Nucleic Acids Res 29:E21.

Ryu JM, Lee MY, Yun SP, Han HJ. 2010. High glucose regulates cyclin D1/E of human mesenchymal stem cells through TGF-beta1 expression via Ca2+/PKC/MAPKs and PI3K/Akt/mTOR signal pathways. J Cell Physiol 224:59–70.

San Martin IA, Varela N, Gaete M, Villegas K, Osorio M, Tapia JC, Antonelli M, Mancilla EE, Pereira BP, Nathan SS, Lian JB, Stein JL, Stein GS, van Wijnen AJ, Galindo M. 2009. Impaired cell cycle regulation of the osteoblast-related heterodimeric transcription factor Runx2-Cbfbeta in osteosarcoma cells. J Cell Physiol 221:560–571.

Semenza GL. 2003. Targeting HIF-1 for cancer therapy. Nat Rev Cancer 3: 721–732.

Shen R, Wang X, Drissi H, Liu F, O'Keefe RJ, Chen D. 2006. Cyclin D1-cdk4 induce runx2 ubiquitination and degradation. J Biol Chem 281:16347–16353.

Sun L, Vitolo M, Passaniti A. 2001. Runt-related gene 2 in endothelial cells: Inducible expression and specific regulation of cell migration and invasion. Cancer Res 61:4994–5001.

Sun L, Vitolo M, Qiao M, Anglin I, Passaniti A. 2004. Regulation of TGFß1-mediated growth inhibition and apoptosis by RUNX2 isoforms. Oncogene 23:4722–4734.

Tsuji K, Komori T, Noda M. 2004. Aged mice require full transcription factor, Runx2/Cbfa1, gene dosage for cancellous bone regeneration after bone marrow ablation. J Bone Miner Res 19:1481–1489.

Vander Heiden MG, Cantley LC, Thompson CB. 2009. Understanding the Warburg effect: The metabolic requirements of cell proliferation. Science 324:1029–1033.

Vitolo MI, Anglin IE, Mahoney WM, Jr, Renoud KJ, Gartenhaus RB, Bachman KE, Passaniti A. 2007. The RUNX2 transcription factor cooperates with the YES-associated protein, YAP65, to promote cell transformation. Cancer Biol Ther 6:856–863.

Westendorf JJ, Zaidi SK, Cascino JE, Kahler R, van Wijnen AJ, Lian JB, Yoshida M, Stein GS, Li X. 2002. Runx2 (Cbfa1, AML-3) interacts with histone deacetylase 6 and represses the p21(CIP1/WAF1) promoter. Mol Cell Biol 22:7982–7992.

Zelzer E, Glotzer DJ, Hartmann C, Thomas D, Fukai N, Soker S, Olsen BR. 2001. Tissue specific regulation of VEGF expression during bone development requires Cbfa1/Runx2. Mech Dev 106:97–106.